JOURNAL of the MEXICAN CHEMICAL SOCIETY

https://www.jmcs.org.mx/

Article

Open Access

J. Mex. Chem. Soc. **2026**, *70(1):e2489*

Received May 24th, 2025
Accepted October 15th, 2025

http://dx.doi.org/10.29356/jmcs.v70i1.2489
e-location ID: 2489

Keywords:
Dithiophosphonates; cholesteryl complexes; organotin; X-ray single crystal; complex biological activity

Palabras clave:
Ditiofosfonatos; complejos con colesterilo; organoestaño; rayos X de monocristal; actividad biológica

***Corresponding author:**
Gabriela Vargas-Pineda
email: dgaby@uaem.mx
Raymundo Cea-Olivares
email: cea@unam.mx

ISSN-e 2594-0317

Tri-Organotin(IV) Coordination Compounds Derived from a Cholesteryl Dithiophosphonate Ligand. Synthesis, Characterization, Structure, and Antibacterial Evaluation

Perla Román-Bravo[1], Gabriela Vargas-Pineda[1*], Fernando Carvajal-Román[1], Marcela López-Cardoso[1], Macdiel Acevedo-Quiroz[2], Patricia Alvarez-Fitz[3], Raymundo Cea-Olivares[4*]

[1]Centro de Investigaciones Químicas. IICBA, Universidad Autónoma del Estado de Morelos. Av. Universidad 1001, 62209 Cuernavaca, Morelos, México.
[2]Departamento de Ingeniería Química y Bioquímica. Tecnológico Nacional de México/IT de Zacatepec, Calzada Tecnológico No. 27, Col. Centro, 62780, Zacatepec, Morelos, México.
[3]Laboratorio de Toxicología, CONACYT-Universidad Autónoma de Guerrero, 39090 Chilpancingo, Guerrero, México.
[4]Instituto de Química, Universidad Nacional Autónoma de México, Circuito Exterior, Ciudad Universitaria, 10810, Ciudad de México, México.

Abstract. Among the dithio-organophosphorus metal coordination compounds, dithiophosphonates have received significantly less attention than dithiophosphates and dithiophosphinates. This is partly due to the inherent difficulties in synthesizing phosphonates. Herein, we report the synthesis and characterization of four new organotin(IV) dithiophosphonate coordination compounds, bearing an O-cholesteryl substituent on phosphorus: $[Me_3Sn\{S_2P(O\text{-cholesteryl})(4\text{-}MeOC_6H_4)\}]$ **(2)**, $[Bu_3Sn\{S_2P(O\text{-cholesteryl})(4\text{-}MeOC_6H_4)\}]$ **(3),** $[Cy_3Sn\{S_2P(O\text{-cholesteryl})(4\text{-}MeOC_6H_4)\}]$ **(4),** $[Ph_3Sn\{S_2P(O\text{-cholesteryl})(4\text{-}MeOC_6H_4)\}]$ **(5).** These compounds were obtained through the reaction between the

J. Mex. Chem. Soc. **2026**, *70(1):e2489*
Regular Issue

ISSN-e 2594-0317

triethylammonium salt of *O*-3-*β*-cholest-5-en-3-yl)(4-methoxyphenyl)dithiophosphonate (1) and the corresponding triorganotin(IV) chlorides. The compounds were characterized using elemental analysis, IR spectroscopy, and NMR spectroscopy (^{1}H, ^{13}C, ^{31}P, and ^{119}Sn). Infrared spectra (solid-state) suggest that the Sn(IV) is coordinated in an anisobidentate mode. In solution, the ^{119}Sn NMR chemical shifts indicate tetracoordination for 2 and 4 and pentacoordination for 3 and 5. Single-crystal X-ray analysis of 5 revealed an anisobidentate coordination mode of the dithiophosphonate and a highly distorted trigonal bipyramidal geometry around Sn(IV), closer to a trigonal bipyramid than to a square pyramid. The phosphorus atom is chiral and adopts the relative configuration R. The antibacterial test indicates that compound 5 exhibits antibacterial activity, while the others show no inhibition against any of the bacterial strains used.

Resumen. Dentro de los compuestos metálicos de coordinación conteniendo ligantes ditio-organofosforados, los ditiofosfonatos han recibido significativamente mucha menos atención que los bien estudiados ditiofosfinatos y ditiofosfatos. Lo anterior es parcialmente debido a las inherentes mayores dificultades sintéticas de los ditiofosfonatos. En esta investigación informamos la síntesis y caracterización de cuatro nuevos compuestos de coordinación de organoestaño(IV) con un ligante ditiofosfonato, conteniendo *O*-colesterilo. Los compuestos de organoestaño (IV) sintetizados son: [$Me_3Sn\{S_2P$(O-colesteril)(4-$MeOC_6H_4$)}] (2), [$Bu_3Sn\{S_2P$(O-colesteril)(4-$MeOC_6H_4$)}] (3), [$Cy_3Sn\{S_2P$(O-colesteril)(4-$MeOC_6H_4$)}] (4), [$Ph_3Sn\{S_2P$(O-colesteril)(4-$MeOC_6H_4$)}] (5). La síntesis se llevó a cabo a través de la reacción entre la sal de trietilamonio del *O*-3-*β*-colest-5-en-3-yl)(4-metoxifenil)ditiofosfonato (1) y los correspondientes cloruros de triorganoestaño(IV). Los compuestos obtenidos fueron caracterizados por análisis elemental, espectroscopia IR y RNM (^{1}H, ^{13}C, ^{31}P, y ^{119}Sn). Los espectros infrarrojos (estado sólido) sugieren que el Sn(IV) se encuentra coordinado al ligante en un modo anisobidentado, mientras que en solución los desplazamientos químicos de ^{119}Sn RNM indican tetracoordinación para 2 y 4 y pentacoordinación para 3 y 5. El análisis por rayos X de monocristal de 5 revela un modo de coordinación anisobidentado del ditiofosfonato y una geometría trigonal bipiramidal altamente distorsionada alrededor del Sn(IV), la cual es más cercana a una bipirámide trigonal que a una pirámide cuadrada, donde el átomo de fósforo es quiral y asume la configuración relativa *R*. Las pruebas antibacterianas indican que el compuesto 5 exhibe actividad antibacteriana, mientras que los demás no muestran inhibición contra ninguna de las cepas utilizadas.

Introduction

1,1-dithiolates are anionic ligands in which two sulfur atoms are bonded to a nonmetal center (e.g., carbon, silicon, and phosphorus), including xanthates, dithiocarboxylates, and dithiocarbamates. In the case of phosphorus, compounds such as dithiophosphates, dithiophosphinates, and dithiophosphonates form metal complexes that are notable for their structural diversity and wide range of applications. These include their use as antioxidant additives, pesticides, metal extraction reagents, flotation agents in mining, and pharmaceutical agents. [1] These complexes exhibit a variety of coordination patterns where the ligand most commonly acting as monodentate or bidentate donors. However, more complex coordination modes also exist, such as bimetallic biconnective, triconnective, and bridging configurations. Some ligands can form clusters, including trimetallic triconnective and tetrametallic tetraconnective systems. In the bidentate complexes, the coordination can be symmetric (isobidentate) or asymmetric (anisobidentate), while the monodentate coordination is relatively rare [2].

The metal coordination chemistry of the dithiophosphate and dithiophosphinate ligands is well known. However, the coordination chemistry of dithiophosphonate ligands $[(R^*)(RO)PS_2]^-$ has been far less studied. This may be due to the greater synthetic challenges associated with the synthesis of dithiophosphonates. These ligands are mainly obtained via the reaction of Lawesson´s dimer with primary or secondary alcohols, a method that enables the preparation of structurally diverse dithiophosphonate derivatives.

Currently, most reported dithiophosphonate metal complexes involve only a limited number of metals and a narrow range of -OR substituents. Consequently, there are significant opportunities for the synthesis and emerging applications of these complexes. The reactivity, hydrolytic stability, and potential toxicity of 1,1-dithiophosphonate coordination compounds are expected to be similar to those of the

http://dx.doi.org/10.29356/jmcs.v70i1.2489

J. Mex. Chem. Soc. **2026**, *70(1):e2489*
Regular Issue

ISSN-e 2594-0317

dithiophosphinate and dithiophosphate analogs. Nonetheless, dithiophosphonates exhibit unique features that offer significant potential. These include the wide variety of derivatives accessible through the use of different alcohols, allowing for tailored design of ligands with specific steric and solubility properties, as well as the inclusion of biologically relevant functional groups.

The asymmetric nature of the dithiophosphonate ligands favors the formation of isomers, unlike their symmetric analogs. Consequently, dithiophosphonates have been considered "an emerging and versatile ligand class" [3].

Recently, there has been a significant increase in the applications of the 1,1-dithiophosphonate coordination compounds. These include their catalytic activity in nanoclusters for decarboxylative acyl arylation and electrochemical hydrogen evolution [4], use as anticorrosive agents [5], and evaluation in cytotoxic assays [6]. Additionally, the range of metals has been extended to include rare earth elements [7].

Despite the possibility of obtaining ligands with a great variety of -OR groups, the number of known dithiophosphonate ligands is limited. In the case of groups containing biological-active moieties, they are restricted to -O-monoterpenols [8] and -O-cholesteryl. The latter has been used in the synthesis of dithio-heterocycles of As(III) and Sb(III) [9]. The structural and functional implications of Sn(IV) organometallic complexes, including those with dithiophosphorus ligands, are well known in the field of medicine [10]. However, organotin dithiophosphonate compounds are still extraordinarily scarce [8,11]. Therefore, we consider it important to extend the study of organotin(IV) dithiophosphonates to include ligands bearing the -O-cholesteryl group. Herein, we report the synthesis and characterization of four new triorganotin(IV) dithiophosphonates, including the single-crystal X-ray structure determination of one compound. In addition, we present bacterial inhibition studies.

The -O-cholesteryl substituent was chosen due to its biological relevance. Cholesteryl is involved in multiple biological processes and is an essential cellular component of cell membranes and signaling pathways. Due to its high steric bulk and hydrophobic character, it can significantly influence solubility, biological interactions, and coordination geometry [12].

Experimental

Materials and methods

All reagents used in the synthesis of the compounds were commercially sourced and used without further purification. Elemental analyses were conducted using a Thermo Scientific Flash 2000 analyzer. Infrared spectra were recorded on a Nicolet 6700 FT-IR spectrophotometer within the range of 4000−500 cm^{-1} using the Smart ITR accessory equipped with a diamond ATR crystal.

The NMR spectra were obtained using a JEOL JMS 700 and a Bruker Avance III HD 500 MHz spectrometer, with $CDCl_3$ or CD_3OD as the solvent; the chemical shifts are expressed in parts per million (ppm), while J values are reported in hertz (Hz). The triethylammonium salt of the ligand was synthesized following a previously reported method [9,13], and characterized by IR, ^{1}H, ^{13}C, ^{119}Sn, and ^{31}P NMR spectroscopy.

Single-crystal X-ray diffraction studies

An Agilent SuperNova, Dual, Cu at zero, EosS2 with a CCD area detector (λCuKα=1.54184 Å, monochromator: graphite) was used to perform the single-crystal X-ray diffraction structural analysis of compound **5.** CrysAlisPro (Agilent Technologies) was used for structural solutions, refinement, and data output [14]. The frames were collected at T=100 K. The measured intensities were diminished to F2 and adjusted for absorption using multiscan empirical absorption correction with spherical harmonics, as implemented in the SCALE3 ABSPACK scaling method. Corrections were implemented for the Lorentz and polarization effects. Non-hydrogen atoms underwent anisotropic refinement, and C-H hydrogen atoms were positioned based on geometric calculations and improved using a riding model, wherein each H atom was assigned a fixed isotropic displacement parameter equivalent to 1.2 Ueq of its corresponding C atom (1.5 Ueq for the methyl groups). The crystallographic data for the structure of **5** are stored at the Cambridge Crystallographic Data Centre (CCDC), located at 12 Union Road, Cambridge CB21EZ, UK. A complimentary copy of the data can be requested by referencing deposit number CCDC 2393584.

http://dx.doi.org/10.29356/jmcs.v70i1.2489

J. Mex. Chem. Soc. **2026**, *70(1):e2489*
Regular Issue

ISSN-e 2594-0317

Synthesis triethylammonium O-3-β-cholest-5-en-3-yl)(4-methoxyphenyl)dithiophosphonate salt (1)

A mixture of Lawesson's reagent (1.49 g, 3.7 mmol) and cholesterol (2.86 g, 7.4 mmol) in toluene (40 mL) was refluxed for five hours. The resulting solution was cooled to room temperature, stirred for 30 min, and then triethylamine (0.50 g, 5.0 mmol) was added dropwise to the solution. The mixture was stirred for one more hour. The solvent was then removed under reduced pressure, and the resulting white solid was recrystallized from a dichloromethane/hexane mixture.

Synthesis of compounds 2-5

General synthetic procedure

Compounds **2-5** were synthesized by reacting triethylammonium-O-3*β*-cholest-5-en-3-yl)(4-methoxyphenyl) dithiophosphonate salt (**1**) with the respective triorganotin (IV) chlorides in a 1:1 molar ratio at room temperature. (Scheme 1). In all cases, 0.25 g of (**1**) was added slowly to the respective R_3SnCl solutions in 20 mL of methanol and stirred for 48 h. Subsequently, the solvent was evaporated under low pressure. The obtained solids were dissolved in 20 mL dichloromethane and filtered. The solvent was then removed again, resulting in the formation of white solids, which were recrystallized from a mixture of dichloromethane and hexane. The corresponding spectra for compounds 2-5 are found in the Supplementary Information section.

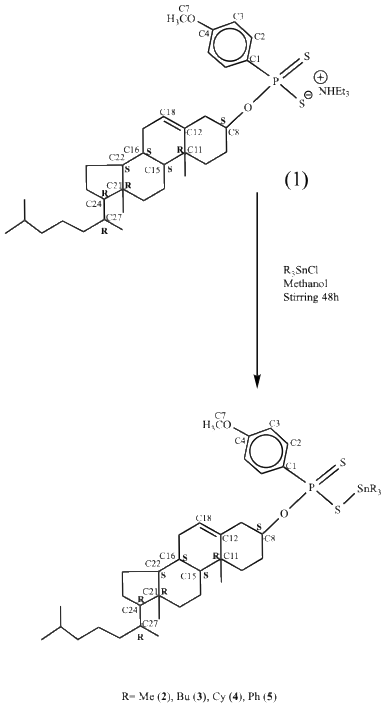

Scheme 1. Synthetic procedure for compounds **2-5**

[$Me_3Sn\{S_2P$(O-cholesteryl)(4-$MeOC_6H_4$)}] **(2).** Yield 63 %. M. p. 137-138 ºC. IR *ν* (cm^{-1}). *ν*(C–H) 2935, *ν*(C=C) 1592, *ν*(C–O) 1109, ν(P-O) 1028, ν(S=P) 636, 548. ^{1}H NMR (400 MHz, $CDCl_3$, δ = ppm) = 7.9 ppm (dd, 2H, ^{3}*J*HP 12.0 Hz, ^{3}*J*HH 8.0 Hz), 6.7 (dd, 2H, ^{4}*J*HP 4.0 Hz, ^{3}*J*HH 8.0), 5.1 (m,1H), 4.1 (m, 1H), 3.7 (s,3H), 2.5-0.5 (m, 52H, cholesteryl and $Sn(CH_3)_3$).^{13}C NMR (125 MHz, $CDCl_3$, δ = ppm) = 161.0 (C-4), 141.2 (C-12), 136.0 (C-1, ^{1}*J*CP 110.0 Hz), 132.3 (C-2, ^{2}*J*CP 13.0 Hz), 121.7 (C-18), 113.0 (C-3, ^{3}*J*CP 12.0 Hz), 75.6 (C-8 , ^{2}*J*CP 8.0 Hz), 55.4 (C-8), C-cholesteryl: 56.9, 56.3, 52.3, 42.5, 40.5, 39.9, 39.7, 37.4, 36.6, 36.3, 35.9, 32.1, 32.0, 30.0, 28.4, 28.1, 24.4, 24, 22.9, 22.7, 21.2, 19.4, 18.9, 12.0, 28.4, 28.1, 24.4, 24, 22.9, 22.7, 21.2, 19.4, 18.9, 12, -1.5 (CH_3Sn, ^{1}*J*SnC 395.5 Hz). ^{119}Sn NMR (161 MHz, $CDCl_3$, δ = ppm) = 99.2. ^{31}P NMR (161 MHz, $CDCl_3$, δ = ppm) = 91.8. Anal Calc. (%) for $C_{37}H_{61}O_2PS_2Sn$ (751.70): C, 59.12; H, 8.18, S, 8.53%; Found: C, 58.11; H, 8.009, S, 7.945.

http://dx.doi.org/10.29356/jmcs.v70i1.2489

J. Mex. Chem. Soc. **2026**, *70(1):e2489*
Regular Issue

ISSN-e 2594-0317

[$Bu_3Sn\{S_2P(O\text{-cholesteryl})(4\text{-}MeOC_6H_4)\}$] **(3).** Yield 54 %. M. p. 176-177 ºC. IR *v* (cm^{-1}). *v*(C–H) 2935, *v*(C=C) 1592, *v*(C–O) 1109, ν(P-O) 1028, ν(S=P) 624, 534. ^{1}H NMR (400 MHz, $CDCl_3$, δ = ppm) = 7.9 ppm (dd, 2H, ^3JHP 12.0 Hz, ^3JHH 8.0 Hz), 6.8 (dd, 2H, ^4JHP 4.0 Hz, ^3JHH 8.0), 5.4 (m,1H), 4.47 (m, 1H), 3.8 (s,3H), 2.5-0.5 (m, 70H, cholesteryl, Sn(n-butyl$_3$)$_3$). ^{13}C NMR (125 MHz, $CDCl_3$, δ = ppm) = 162.0 (C-4), 141.2 (C-12), 132.3 (C-2, ^2JCP 13.0 Hz), 130.0 (C-1, ^1JCP 110.0 Hz), 122.8 (C-18), 112.9 (C-3, ^3JCP 12.0 Hz), 75.6 (C-8), 55.4 (C-7), C-nButyl: 17.1, 28.2, 27.2, 13.8, C-cholesteryl: 56.9, 56.3, 52.3, 42.5, 40.5, 39.9, 39.7, 37.4, 36.6, 36.3, 35.9, 32.1, 32.0, 30, 28.4, 28.1, 24.4, 24, 22.9, 22.7, 21.2, 19.4, 18.9, 12. ^{119}Sn NMR (161 MHz, $CDCl_3$, δ = ppm) = -175.2. ^{31}P NMR (161 MHz, $CDCl_3$, δ = ppm) = 94.4. Anal Calc. (%) for $C_{64}H_{79}O_2PS_2Sn$ (877.94): C, 62.93, H, 9.07, S, 7.3 %; Found: C, 61.901, H, 9.25, S,7.27.

[$Cy_3Sn\{S_2P(O\text{-cholesteryl})(4\text{-}MeOC_6H_4)\}$] **(4).** Yield 80 %. M. p. 115-116 ºC. IR *v* (cm^{-1}). *v*(C–H) 2935, *v*(C=C) 1592, *v*(C–O) 1109, ν(P-O) 1028, ν(S=P) 620, 533. ^{1}H NMR (400 MHz, $CDCl_3$, δ = ppm) = 8.0 ppm(dd,2H, ^3JHP 12.0 Hz and ^3JHH 8.0 Hz), 6.8 (dd,2H, ^4JHP 4.0 Hz, ^3JHH 8.0), 5.3 (m,1H), 4.3 (m, 1H), 3.8 (s,3H), 2.5-0.5 (m, 76H, cholesteryl, Sn(Cy_3)$_3$). ^{13}C NMR (125 MHz, $CDCl_3$, δ = ppm) = 161.0 (C-4), 141.2 (C-12), 132.0 (C-1, ^1JCP 110.0 Hz), 132.1 (C-2, ^3JCP 13.0 Hz), 121.8 (C-18), 123.0 (C-3, ^3JCP 12.0 Hz), 75.6 (C-8), 55.4 (C-7), C-Cyclohexyl 27.1, 34.6, 32.3, 29.4, C-cholesteryl: 56.9, 56.3, 52.3, 42.5, 40.5, 39.9, 39.7, 37.4, 36.6, 36.3, 35.9, 32.1, 32.0, 30, 28.4, 28.1, 24.4, 24, 22.9, 22.7, 21.2, 19.4, 18.9, 12. ^{119}Sn NMR (161 MHz, $CDCl_3$, δ = ppm) = 21.2. ^{31}P NMR (161 MHz, $CDCl_3$, δ = ppm) = 94.6. Anal Calc. (%) for $C_{52}H_{85}O_2PS_2Sn$ (956.05): C, 65.33; H, 8.96, S. 6.71 %; Found: C, 62.11; H, 8.54, S, 6.40.

[$Ph_3Sn\{S_2P(O\text{-cholesteryl})(4\text{-}MeOC_6H_4)\}$] **(5).** Yield 76 %. M. p. 150-151 ºC. IR *v* (cm^{-1}). *v*(C=C–H) 3035, *v*(C–H) 2935, *v*(C=C) 1592, *v*(C–O) 1109, ν(P-O) 1028, ν(S=P) 618, 530. ^{1}H NMR (400 MHz, $CDCl_3$, δ = ppm) = 7.8 ppm (dd, 2H, ^3JHP 12.0 Hz, ^3JHH 8.0 Hz), 6.8 (dd,2H, ^4JHP 4.0 Hz, ^3JHH 8.0), 5.2 (d,1H, ^3JHH 8.0 Hz), 4.3 (m, 1H), 3.8 (s,3H), 7.3-7.7 (m,15H, Sn(Ph_3)$_3$), 2.5-0.5 (m, 76H, cholesteryl). ^{13}C NMR (125 MHz, $CDCl_3$, δ = ppm) = 161.0 (C-4), 141.2 (C-12), 136.0 (C-1 ^1JCP 110.0 Hz), 132.3 (C-2 ^2JCP 13.0 Hz), 121.8 (C-18), 75.6 (C-8), 55.4 (C-7), C-Phenyl 138.9, 137.2, 129.8, 128.9, C-cholesteryl: 56.9, 56.3, 52.3, 42.5, 40.5, 39.9, 39.7, 37.4, 36.6, 36.3, 35.9, 32.1, 32.0, 30, 28.4, 28.1, 24.4, 24, 22.9, 22.7, 21.2, 19.4, 18.9, 12. ^{119}Sn NMR (161 MHz, $CDCl_3$, δ = ppm) = -93.7. ^{31}P NMR (161 MHz, $CDCl_3$, δ = ppm) = 89.6. Anal Calc. (%) for $C_{52}H_{67}O_2PS_2Sn$ (937.91): C, 66.59; H, 7.20, S. 6.84 %; Found: C, 64.74; H, 6.89, S, 6.503.

Antibacterial activity

Microorganism and inoculum preparation

This study employed six American Type Culture Collection (ATCC) reference strains, including two Gram-negative bacteria: *Escherichia coli* (ATCC 35218 and ATCC 25922), and four Gram-positive strains: *Staphylococcus aureus* (ATCC 25923), *Enterococcus faecalis* (ATCC 29212), *Enterobacter cloacae* (ATCC 700323), and *Salmonella dublin* (ATCC 9676). In addition, three clinically isolated multi-drug-resistant strains were used: one Gram-negative: *Escherichia coli* and two Gram-positive (*Staphylococcus haemolyticus* and *Staphylococcus hominis)*.

All bacterial strains were maintained on Mueller-Hinton (MH) agar at 4 °C until use. For experimental procedures, bacteria were inoculated into 4 mL of MH broth and incubated at 37 °C for 18 hours. The bacterial suspensions were then adjusted to a 0.5 McFarland standard to ensure uniform cell density.

Minimum Inhibitory Concentration (MIC) determination

Antibacterial testing was carried out using the serial microdilution method [15]. The test compounds and the standard antibiotic kanamycin were dissolved in a mixture of 20 % DMSO in sterile water. These solutions were serially distributed into the wells of a microplate, covering a concentration range of 12.5 to 100 µg/mL. Five microliters of bacterial culture were added to each well. The microplate was incubated at 37 °C for 24 hours. After incubation, 3-(4,5-dimethylthiazol-2-yl)-2,5-diphenyl-2H-tetrazolium bromide (MTT, 0.5 mg/mL) was added to each well. The appearance of violet-blue color indicated cell viability. The minimum inhibitory concentration (MIC) was defined as the lowest concentration of the sample that did not result in a violet-blue color, based on the average of three independent assays.

http://dx.doi.org/10.29356/jmcs.v70i1.2489

J. Mex. Chem. Soc. **2026**, *70(1):e2489*
Regular Issue

ISSN-e 2594-0317

Results and discussion

Synthesis and spectroscopy characterization

Compounds **2**–**5** are white solids that are stable at room temperature, soluble in dichloromethane, and insoluble in ethanol or hexane. The yields ranged from 54 % to 80 %. The organotin(IV) complexes were characterized using elemental analysis, infrared spectroscopy, and multinuclear NMR spectroscopy (^{1}H, ^{13}C, ^{31}P, and ^{119}Sn). The structure of **5** was determined using single-crystal X-ray diffraction.

The formation of compounds **2**-**5** was confirmed by IR, ^{31}P, and ^{119}Sn NMR spectroscopy (Table 1). The IR spectra of compounds **2**-**5** exhibit bands at $\bar{\nu}$ 1600, 1150, and 1000 cm^{-1}, which correspond to the vibrations C=C, C–O, and P–O, respectively, and are similar to those of the ammonium salt of the ligand. Additionally, two bands appear for the PS_2 group in the asymmetric region at $\bar{\nu}$ 618–636 cm^{-1} and the symmetric region at $\bar{\nu}$ 530–548 cm^{-1}, due to stretching vibrations. According to Haiduc [16], a separation of 87 cm^{-1} between these bands is consistent with an anisobidentate coordination mode.

Table 1. Selected IR (cm^{-1}), NMR ^{31}P (ppm) and NMR ^{119}Sn (ppm) spectroscopy data for compounds **1**-**5**.

	1	**2**	**3**	**4**	**5**
ν(CH)	2958	2955	2941	2965	2960
ν[(P)-O-C]	1150	1180	1249	1250	1249
ν[P-O-(C)]	1000	954	966	968	990
$\nu(P\text{-}S)_{asym}$	624	636	621	620	618
$\nu(P\text{-}S)_{sym}$	552	548	534	533	530
δ ^{31}P δ ^{119}Sn	105.8 -------	91.8 99.2	94.4 -175.2	94.6 21.2	89.6 -93.7

The ^{1}H and ^{13}C NMR spectra show resonances with integrals and chemical shifts consistent with the proposed structures. The ^{31}P NMR spectra indicate the presence of a single, pure compound, as they exhibit only one signal for each of the four complexes (**2**: 91.8 ppm, **3**: 94.4 ppm, **4**: 94.6 ppm, and **5**: 89.6 ppm). These signals are displaced to a higher field compared to the ligand salt **1** (105.8 ppm) and are indicative of a bidentate coordination mode in the solution of the Sn(IV) compounds [17]. The observation of a single ^{31}P resonance is consistent with rapid exchange between coordination modes and/or the presence of a single diastereoisomer in solution. The ^{119}Sn NMR chemical shifts are influenced by various factors, including the electronegativity of the ligands, the angle around the metal center, and the presence of voluminous and electronegative substituents. Due to the large spectral window, ^{119}Sn NMR is an appropriate technique for determining the Sn coordination number in solution [28]. Generally, as the coordination number increases, the ^{119}Sn NMR shift moves to lower frequencies. Based on the reported values [19], compounds **3** and **5** can be considered as pentacoordinate in solution, while **2** and **4** as tetracoordinate

Crystal structure description

Single crystals of compound **5** were grown at room temperature by slow evaporation from a dichloromethane-methanol solution. The most relevant crystallographic data are listed in Table 2. Selected bond lengths (Å) and bond angles (°) for **5** are given in Table 3. Fig. 1 shows the asymmetric unit of **5** with the corresponding atom numbering scheme. In **5,** the phosphorus atom has a distorted tetrahedral geometry with angles X-P-X (X = S, O, or C) ranging from 103.91(11)° to 116.10(11)°. In compound **5**, the phosphorus atom is chiral; given the known configuration of the stereogenic centers in the cholesteryl fragment, the phosphorus atom adopts the relative configuration *R*.

J. Mex. Chem. Soc. **2026**, *70(1):e2489*
Regular Issue

ISSN-e 2594-0317

Table 2. Selected crystallographic data for compound **5**.

Formula	$C_{52}H_{67}O_2PS_2Sn$
MW (g mol^{-1})	937.83
Crystal system	Monoclinic
Space group	C2
T (K)	100
Cell parameters	
A (Å)	17.8515(3)
B (Å)	9.63816(14)
C (Å)	28.0530(4)
β *(°)*	94.8853(13)
Volume (Å^3)	4809.13(13)
Z	4
ρ_{calc} (g/cm^3)	1.295
μ/mm^{-1}	5.635
Data collection	
2Θ limits (°)	6.324 – 145.258
Radiation	CuKα (λ = 1.54184)
Number of reflections collected	8901
Number of independent reflections R_{int}	5949 (0.0179)
Data/restraints/parameters	5949/1/529
Refinement	
Goodness-of-fit on F^2	1.037
R^{ab}	0.0240
R_w^{cd}	0.0637
Goodness-of-fit	1.037
$\Delta\rho_{min}$ (eA^{-3})	-0.62
$\Delta\rho_{max}$ (eA^{-3})	0.65
Flack parameter	-0.005(4)

http://dx.doi.org/10.29356/jmcs.v70i1.2489

J. Mex. Chem. Soc. **2026**, *70(1):e2489*
Regular Issue

ISSN-e 2594-0317

The tin atom in **5** is bonded to three carbon atoms from the phenyl groups and two sulfur atoms from the dithiophosphonate in an anisobidentate chelating mode [20]. The Sn(1)–S(1) bond distance of 2.4414(9) Å is consistent with the Sn–S single bond distance, and the Sn(1)···S(2) distance of 3.6025(8) Å, is longer than the sum of the covalent radii [Σr_{cov} (Sn, S) = 2.44 Å] [20] but shorter than the sum of the van der Waals radii [Σ_{vdW} (Sn, S) = 3.97 Å] [21]. Therefore, this last bond can be described as a secondary bond that influences the local geometry of the Sn atom along the path from tetracoordinate to pentacoordinate geometry, leading to a highly distorted geometrical arrangement. The degree of trigonal distortion (τ) for a five-coordinate geometry, as calculated by Addison's method [23], is 0.82, indicating that the coordination polyhedron is closer to a trigonal bipyramid (τ = 1) than to a square pyramid (τ = 0). The apical positions are occupied by the S(2) and C(41) atoms attached to the tin atom. The angle involving these atoms and the metal center corresponds to 162.56 (12)º for S(2)···Sn(1)-C(41), as shown in Fig. 2. Additionally, the Sn(1)–S(1) bond 2.4414(9) Å is associated with the elongated P(1)–S(1) bond 2.0847(11) Å. The same situation is observed for the Sn(1) ···S(2) contact 3.6025(8) Å and the short P(1)–(S2) 1.9394 Å. This trend is common for asymmetrically coordinating ligands [24]. Intramolecular interactions O (1)···H(2)-C(2) 2.397(3) Å and (S2)···H(40)-C(40) 3.0106(9) are observed (Fig. 2), which are not present in the triethylammonium salt of the ligand [25].

Table 3. Selected bond lengths (Å) and bond angles (º) for **5**.

Bond Lengths	
Sn(1)-S(1)	2.4414(9)
Sn(1)-S(2)	3.6025(8)
P(1)-S(1)	2.0847(11)
P(1)-S(2)	1.9394(13)
P(1)-C(1)	1.794(4)
P(1)-O(1)	1.588(2)
Sn(1)-C(35)	2.146(3)
Sn(1)-C(41)	2.147(3)
Sn(1)-C(47)	2.144(4)
C(2)-H(2)···O(1)	2.397(3)
C(40)-H(40) ···(S2)	3.010(9)
Bond angles	
S(1)-Sn(1)-S(2)	64.41(3)
C(35)-Sn(1)-S(1)	109.93(12)
C(41)-Sn(1)-S(1)	98.23(11)
C(47)-Sn(1)-S(1)	113.28(9)
C(41)-Sn(1)-S(2)	162.56(12)
C(47)-Sn(1)-S(2)	83.79(10)

http://dx.doi.org/10.29356/jmcs.v70i1.2489

J. Mex. Chem. Soc. **2026**, *70(1):e2489*
Regular Issue

ISSN-e 2594-0317

Bond angles	
C(35)-Sn(1)-S(2)	75.62(9)
S(2)-P(1)-S(1)	113.56(5)
O(1)-P(1)-S(1)	106.11(10)
C(1)-P(1)-S(1)	103.91(11)
C(1)-P(1)-S(2)	116.10(11)
O(1)-P(1)-S(2)	115.83(11)
O(1)-P(1)-C(1)	99.67(15)

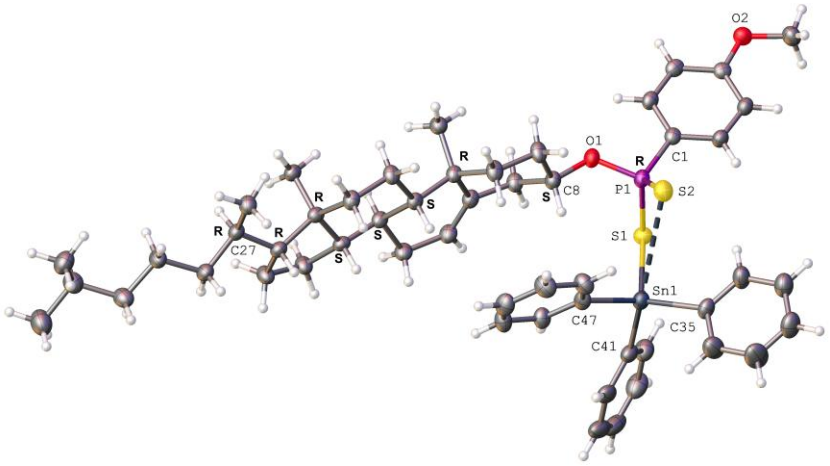

Fig. 1. Asymmetric unit of complex **5**. Displacement ellipsoids are shown at the 50 % probability level, showing the relative configuration of the phosphorus atom.

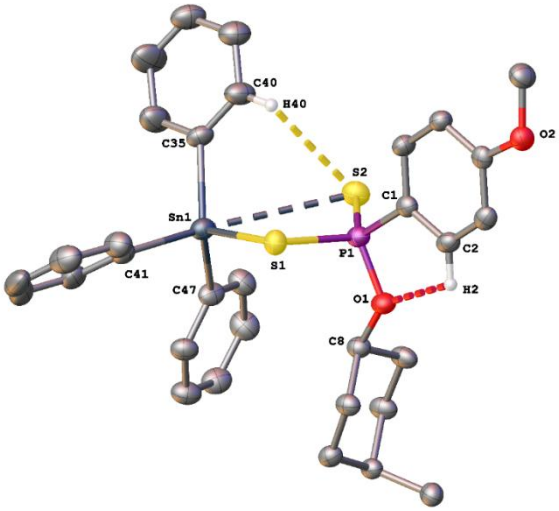

Fig. 2. Distorted trigonal bipyramidal geometry of the Sn atom and intramolecular interactions in **5**. Hydrogen atoms (except C(40)-H(40) and C(2)-H(2)) and some atoms of the cholesteryl moiety have been omitted for clarity.

http://dx.doi.org/10.29356/jmcs.v70i1.2489

J. Mex. Chem. Soc. **2026**, *70(1):e2489*
Regular Issue

ISSN-e 2594-0317

In the crystal structure of compound **5,** the neighboring molecules are interconnected by C-H···S hydrogen bonds, generating chains running along the b-axis. The chains are linked by C-H···C(π) cooperative interactions, which cause the cholesteryl units to adopt an alternating herring-bone arrangement along the two-fold screw axis. (Table 4, Fig. 3).

Table 4. Hydrogen -bond geometry (Å, º).

Interaction	Distance (Å) D-H···A	Distance (Å) H···A	Angle Distance (°) D-H···A	Symmetry operation
C50-H50···S1	3.646	2.994	127.00	x,-1+y,z
C9-H9B···S2	3.538	2.758	136.97	x,-1+y,z
C10-H10A···C3	3.433	2.669	134.18	x,-1+y,z
C49-H49···C6	3.793	2.867	165.49	x,-1+y,z
C7-H7A···S3	3.894	2.984	154.95	x,-1+y,z
C8-H18···S2	3.859	2.737	170.61	-1/2+x,-1/2+y,z
C8-H18···C3	3.469	2.735	121.85	-1/2+x,-1/2+y,z
C8-H18···C4	3.668	2.711	141.72	-1/2+x,-1/2+y,z
C24-H24···S2	3.803	2.909	149.17	1/2+x,1.5+y,z
C36-H36···C39	3.799	2.892	160.21	1/2-x,-1/2+y,1-z

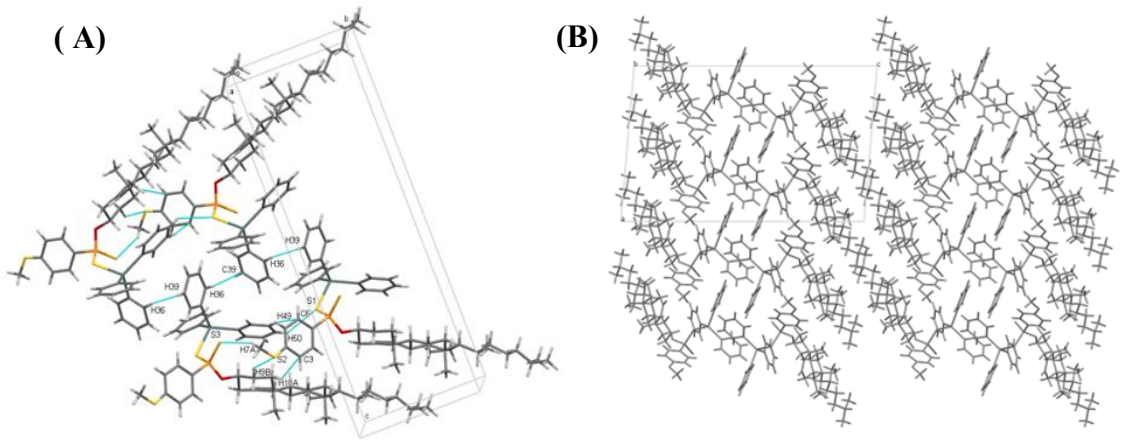

Fig. 3. Fragment of the crystal packing of compound **5. (A)** View along axis a showing the supramolecular network C-H···C(π), C-H···S. **(B)** View along axis b showing the herringbone arrangement along the two-fold screw.

Additional information on the nature of intermolecular interactions was obtained from Hirshfeld surface analysis. The surface was generated using the Crystal Explorer software based on the X-ray structures in the CIF format [26]. The surface was mapped using the d_{norm} function, with three colors indicating different types of interactions: red for attractive, white for neutral, and blue for repulsion. Red regions indicate contacts

http://dx.doi.org/10.29356/jmcs.v70i1.2489

J. Mex. Chem. Soc. **2026**, *70(1):e2489*
Regular Issue

ISSN-e 2594-0317

shorter than the sum of the van der Waals radii with a negative d_{norm}. The opposite is true for blue regions, which represent contact sites longer than the sum of the van der Waals radii, with d_{norm} equal to zero. In compound **5**, red spots on the d_{norm} surface appeared near the C-H groups of the cholesteryl and 4-methoxyphenyl fragments (Fig. 4). This is consistent with the formation of C-H···C(π) interactions.

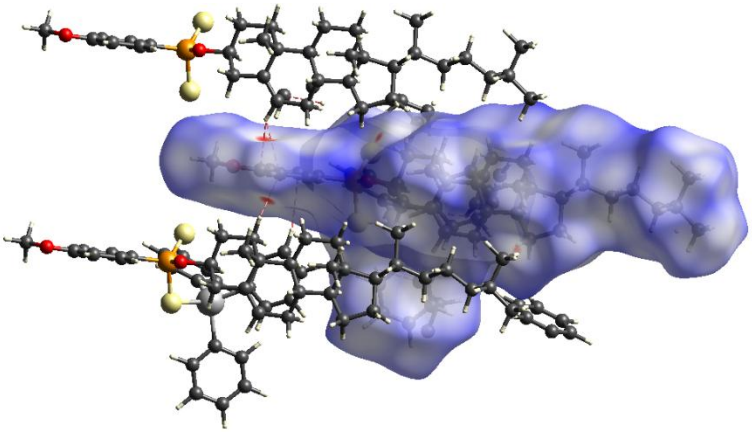

Fig. 4. The Hirshfeld surface mapped with d_{norm} for compound **5.**

Three-dimensional (3D) Hirshfeld surfaces were reduced to two-dimensional (2D) histograms using d_i and d_e distances, which are the distances from the Hirshfeld surface to the nearest nucleus inside and outside the surface, respectively. When the 2D fingerprint plot for compound **5** was partitioned (Fig. **5**), the most abundant contacts were C-H/H-C, H-H, and O-H/H-O, which together account for 17.6-73.1 % of the surface, with an H-H contribution of 2.5 %.

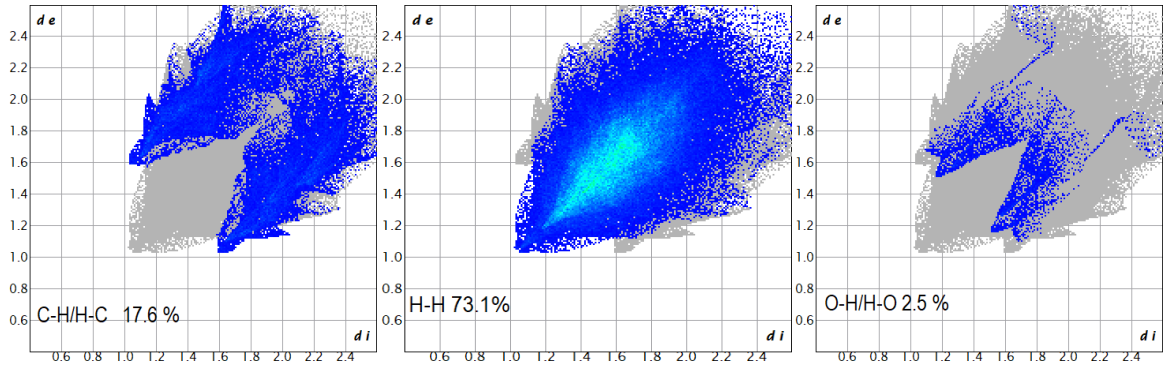

Fig. 5. Representative fingerprint plots for compound **5**.

Antibacterial activity

The *in vitro* antibacterial activity of compounds **2-5** was evaluated by determining their minimum inhibitory concentration (MIC), defined as the lowest concentration of the compound (μM) capable of completely inhibiting microbial growth at 37 °C. The evaluation is detailed in Table 5. Notably, only compound **5** exhibited significant activity against the clinical strain *Staphylococcus hominis*, with an MIC of 52.29 μM. In addition to its higher lipophilicity due to the triphenyl group, the possible causes of the exclusive activity of compound **5** against *S. hominis* may involve the coordination geometry and electronic environment of the Sn(IV) center. These factors likely play a key role in enabling more efficient interactions with biological targets, such as bacterial membranes

J. Mex. Chem. Soc. **2026**, *70(1):e2489*
Regular Issue

ISSN-e 2594-0317

and enzymes, compared to compounds **2**, **3**, and **4**. Furthermore, stability in aqueous media may partly explain this selectivity. The greater structural rigidity and intramolecular interactions observed in **5** could confer superior resistance to hydrolysis or decomposition under the assay conditions, thereby preserving its integrity and enabling antimicrobial activity. Previous studies have reported that coordination geometry and colloidal stability significantly influence the bioactivity of organotin complexes [27].

The lack of antibacterial activity of compounds **2**, **3**, and **4** may be associated with the combined effects of the lower lipophilicity of the alkyl substituents and their different geometries, which may limit intracellular penetration and accumulation [28]. This interpretation is consistent with previous findings for other organometallic complexes, in which the nature of the ligand, steric bulk, and metal coordination govern the selectivity and antimicrobial spectrum [29]. These results highlight the potential of the triphenyl group for the design of organometallic complexes with potent antimicrobial activity, particularly against multidrug-resistant strains such as *S. hominis* [30], a coagulase-negative s*taphylococcus* (CNS) that typically resides on the skin and mucous membranes of healthy individuals. However, *S. hominis* poses a significant threat as a leading cause of bacteremia and catheter-associated infections in vulnerable patients in intensive-care units. The urgent demand for new antimicrobial agents is driven by the widespread resistance of CNS to multiple antibiotics, including penicillinase-resistant glycopeptides such as vancomycin and teicoplanin, as well as oxazolidinones such as linezolid. The efficacy of the complexes evaluated in this study may be limited by their intrinsic hydrophobicity, which is attributable to the cholesteryl substituent, which reduces their solubility in the aqueous medium required for direct microorganism-complex interactions [9].

Table 5. Antibacterial activity of compounds **1**-**5** against ATCC strains and clinical isolates.

Minimum Inhibitory Concentration (µM)									
Compounds	**ATCC Strains**						**Clinical Isolate Strains**		
	Ec1	**Ec2**	**Sa**	**Ef**	**Ecl**	**Sd**	**Sha**	**Sho**	**Ec3**
1	>100	>100	>100	>100	>100	>100	>100	>100	>100
2	>100	>100	>100	>100	>100	>100	>100	>100	>100
3	>100	>100	>100	>100	>100	>100	>100	>100	>100
4	>100	>100	>100	>100	>100	>100	>100	>100	>100
5	>100	>100	>100	>100	>100	>100	>100	52.29	>100
KET	-	-	-	-	-	-	-	-	-
MH	+	+	+	+	+	+	+	+	+

ATCC Strains: Ec1 and Ec2: *Escherichia coli* ATCC 35218 and 25293, respectively; *Staphylococcus aureus* ATCC 25293; Ef: *Enterococcus faecalis* ATCC 29212; Ecl: *Enterobacter cloacae* ATCC 700323; Sd: *Salmonella dublin* ATCC 9626. Clinical isolated strains: Sha: *Staphylococcus haemolyticus*; Sho: *Staphylococcus hominis*; and Ec3: *E. coli*. KET: Kanamycin at 2 µM. MH: Muller-Hinton Medium. +/-: Growth/no normal growth of the strain.

Conclusions

In this article, we extend the knowledge of the coordination chemistry of dithiophosphonates, versatile but understudied ligands. We report the synthesis and antibacterial evaluation of four new tris-organotin (IV) dithiophosphonate complexes bearing a ligand with a biologically active group *O*-3β-cholest-5-en-3-yl)(4-methoxyphenyl)dithiophosphonate. The compounds were fully characterized using standard analytical and spectroscopic techniques. The single-crystal X-ray structure of compound **5**, [$Ph_3Sn[S_2P(O$-cholesteryl(4-$MeOC_6H_4)$)], was obtained, corroborating the anisobidentate mode inferred from IR spectroscopy. The ^{119}Sn

ISSN-e 2594-0317

NMR chemical shifts indicate tetracoordination for compounds **2** and **4** and pentacoordination for compounds **3** and **5**. In compound **5**, the tin atom adopts a markedly distorted trigonal bipyramidal geometry, which is attributable to the steric hindrance of the aromatic rings bound to the tin atom. In the antibacterial assays, **5** exhibited significant activity against *S. hominis*, highlighting the importance of the triphenyl substituent in the design of potent organometallic antimicrobial agents.

Acknowledgements

Part of this research work was carried out for the bachelor´s thesis of Fernando Carvajal-Román, entitled "Caracterización estructural de complejos de triorganoestaño (iv) utilizando un ligante ditiofosfonato con una molécula biológicamente activa (colesterol)", supervised by Dr. Gabriela Vargas-Pineda, which can be found in the repository of the Universidad Autónoma del Estado de Morelos [30].

The authors thank the National Laboratory of Macromolecular Structure Laboratory (LANEM) for the use of their NMR spectrometer.

References

1. (a) Haiduc, I.; Sowerby, D.B. *Polyhedron.* **1995**, *15*, 2469-2521. DOI: https://doi.org/10.1016/0277-5387(95)00554-4. (b) Haiduc, I.; Sowerby, D.B.; Lu, S-F. *Polyhedron.* **1995**, *14*, 3389-3472. DOI: https://doi.org/10.1016/0277-5387(95)00108-5.
2. (a) Haiduc, I. *J. Organomet. Chem.* **2001**, *623*, 298-42. DOI: https://doi.org/10.1016/S0022-328X(00)00677-X. (b) Semeniuc, R.F.; Baum, R.R.; Veach, J.J.; Wheeler, K.A.; Pellechia, P.J. *Inorg. Chim. Acta* **2013**, *400*, 228-238. DOI: https://doi.org/10.1016/j.ica.2013.02.037.
3. van Zyl, W.E.; Woollins, J.D. *Coord. Chem. Rev.* **2013**, *257*, 718-731. DOI: https://doi.org/10.1016/j.ccr.2012.10.010.
4. (a) Yusuf, T.L.; Ogundare, S. A.; Pillay, M. N.; van Zyl, W.E. *Molecules.* **2022**, *27*, 5223. DOI: https://doi.org/10.3390/molecules27165223. (b) Jangid, D.K.; Dastider, S.G.; Biswas, R.; Khirid, S.; Meena, S.; Kumar, P.; Sahoo, S.C.; Verma, V.P.; Makde, R.D.; Kumar, A.; Jangir, R.; Mondal, K.; Haldar, K.K.; Dhayal, R.S. *Inorg. Chem* **2022**, *61*, 13342–13354. DOI: https://doi.org/10.1021/acs.inorgchem.2c01281. (c) Kumar, P.; Khirid, S.; Jangid, D.K.; Nishad, C.S.; Chauhan, P.; Kumari, P.; Meena, S.; Bose, S.K.; Kumar, A.; Banerjee, B.; Dhayal, R.S. *Inorg. Chem.* **2024**, *63*, 13724–13737. DOI: https://doi.org/10.1021/acs.inorgchem.4c02062. (d) Jangid, D. K.; Dastider, S. G.; Mandal, S.; Kumar, P.; Kumari, P.; Haldar, K. K.; Mondal, K.; Dhayal, R.S. *Chem. Eur. J.* **2024**, e202402900. DOI: https://doi.org/10.1002/chem.202402900.
5. Yusuf, T.L.; Quadri, T.W.; Tolufashe, G.F.; Olasunkanmi, L.O.; Ebenso, E. E.; van Zyl, W.E. *RSC Advances* **2020**, *10*, 41967-41982. DOI: https://doi.org/10.1039/D0RA07770D.
6. Sağlam, E.G.; Akkoç, S.; Zorlu, Y.; Bulat, E.; Akgün, A. *Polyhedron,* **2021**, *199*, 115097. DOI: https://doi.org/10.1016/j.poly.2021.115097.
7. Aydin, A.; Dede, B. *Acta Phys. Pol. A* **2023**, *144*, 154-162. DOI: https://doi.org/10.12693/APhysPolA.144.154.
8. Nizamov, I.S.; Yakovlev, A.A.; Nizamov, I.D.; Terenzhev, D.A.; Ivshin, K.A.; Kataeva, O.N.; Shulaeva, M.P.; Pozdeev, O.K. *Appl. Organomet. Chem.* **2018**, *32*, e4320. DOI: https://doi.org/10.1002/aoc.4320.
9. Sosa-García, D.; López-Cardoso, M.; Tlahuext, H.; Vargas-Pineda, G.; Román-Bravo, P.; Villamil-Ramos, R.; Acevedo-Quiroz, M.; Said Razo-Hernández, R.; Gómez-Sandoval, Z.; Alvarez-Fitz, P.; Cea-Olivares, R. *Inorg. Chim. Acta* **2019**, *495*, 118943. DOI: https://doi.org/10.1016/j.ica.2019.05.042.

ISSN-e 2594-0317

10. Jain, V.K. *Coord. Chem. Rev.* **1994**, 135-136, 809-843. DOI: https://doi.org/10.1016/0010-8545(94)80083-9.
11. (a) Fild, M.F.; Krueger, O; Silaghi-Dumitrescu, I.; Thoene, C.; Weinkauf, A. *Phosphorus Sulfur Silicon Relat. Elem.* **2007**, *182*, 2283-2310. DOI: https://doi.org/10.1080/10426500701429122. (b) Hernandez-Galindo, M. del C.; Moya-Cabrera, M.; Jancik, V.; Toscano R.A.; Cea-Olivares R. *J. Organomet. Chem.* **2016**, *813*, 55-60. DOI: https://doi.org/10.1016/j.jorganchem.2016.04.005. (c) Baum, R. R.; Veach, J. J.; Semeniuc, R.F.; Wheeler, K.A.; Pellechia, P.J. *Inorg. Chim. Acta* **2017**, *455*, 52-60. DOI: https://doi.org/10.1016/j.ica.2016.10.006. (d) Nizamov, I.S.; Gabdullina, G.T.; Nizamov, I. D.; Nikitin, Y.N.; Al'metkina, L.A.; Lyubov, R.; Cherkasov, A. *Phosphorus Sulfur Silicon Relat. Elem.* **2010**, *185*, 732-742. DOI: https://doi.org/10.1080/10426500902930142.
12. (a) Ikonen, E. *Nature Reviews Molecular Cell Biology*, **2008,** *9*, 125–138. DOI: https://doi.org/10.1038/nrm2336. (b) Lingwood, D.; Simons, K. *Science,* **2010**, *327*, 46–50. DOI: https://doi.org/10.1126/science.1174621. (c) Simons, K.; Ikonen, E. *Nature*, **1997**, *387* 569–572
13. Van Zyl, W.E.; Fackler J.P. *Phosphorus, Sulfur Silicon Relat. Elem.* **2000** *167* 117-132. DOI: https://doi.org/10.1080/10426500008082393.
14. (a) Agilent, CrysAlis PRO, *Agilent technologies ltd, begbroke*, England. **2014**, (b) Sheldrick, G.M. *Acta Crystallogr. A.*, **2008**, 64, 112-122. DOI: https://doi.org/10.1107/S0108767307043930. (c) Sheldrick G. M. *Acta Crystallogr. C.* **2015**, 71, 3-8. DOI: https://doi.org/10.1107/S2053229614024218. (d) Speck A.L. *Acta Crystallogr. D*. **2009**, *65*, 148-155 DOI https://doi.org/10.1107/s090744490804362x. (e) Westrip, S. P. *J. Appl. Crystallogr*. **2010**, *43*, 920-925. DOI: https://doi.org/10.1107/s0021889810022120.
15. Rios, J.L.; Recio, M.C.; Villar A. *Ethnopharmacol*. **1988**, *23*, 127-149. DOI: https://doi.org/10.1016/0378-8741(88)90001-3.
16. (a) Haiduc, I.; Silaghi-Dumitrescu, I.; Grecu, R.; Constantinescu, R.; Silaghi-Dumitrescu, L. *J. Mol.Struct.* **1984**, *114*, 467–470. DOI: https://doi.org/10.1016/0022-2860(84)87188-4
17. Glidewell, C. *Inorg. Chim. Acta* **1977**, 25, 159-163. DOI https://doi.org/10.1016/S0020-1693(00)95706-2.
18. (a) Martínez García, J.C.; Montes, Tolentino P.; Hernández Ahuactzi, I.F.; Godoy Alcantar C.; Ariza-Castolo, A.; Guerrero Alvarez, J.A. *J. Mol. Struct*. **2020**, *1209*, 127915. DOI: https://doi.org/10.1016/j.molstruc.2020.127915. (b) Wrackmeyer, B. *Annu. Rep. NMR Spectrosc.* **1985**, *16*, 73 (c) Wrackmeyer B., in: *Organotin chemistry in: G.A.* Webb (Ed.), Modern Magnetic Resonance, Springer, Dordrecht, **2008**.
19. (a) Clark, H.C.; Jain, V.K.; Mehrotra, R.C.; Singh, B.P.; Srivastava, G.; Birchall, T. *J. Organomet Chem.* **1985**, *219*, 385-394. DOI: https://doi.org/10.1016/0022-328X(85)87036-4. (b) Otera, J. *J. Organomet. Chem.* **1981**, *221*, 57-61 DOI https://doi.org/10.1016/S0022-328X(00)81028-1.
20. James, B.D.; Magee, R.J.; Patalinghug, W.C.; Skelton, B.W.; White, A.H. *J. Organomet. Chem*. **1994**, *64*, 51-55. DOI: https://doi.org/10.1016/0022-328X(94)88007-7.
21. Cordero, B.; Gómez, V.; Platero-Prats, A.E.; Revés, M.; Echeverría, J.; Cremades, E.; Barragán, F.; Alvarez, S. *Dalton Trans*. **2008**, 2832-2838. DOI: https://doi.org/10.1039/b801115j.
22. Haiduc, I. *Coord. Chem. Rev*. **1997**, *158*, 325-358. DOI: https://doi.org/10.1016/S0010-8545(97)90063-1
23. Addison, A.W.; Rao, T.; Nageswara, R.; Reedijk, J.; Jacobus, V.R.; Verschoor, G.C. *J. Chem. Soc., Dalton Trans.* **1984**, 1349-1356. DOI: https://doi.org/10.1039/DT9840001349.
24. (a) Kumar, S.B.; Chaudhury, M. *J. Chem. Soc. Dalton Trans.* **1992**, 3439-3443. DOI: https://doi.org/10.1039/DT9. (b) Tiekink, E. R. T. *Appl*. *Organomet. Chem*. **2008**, *22*, 533-550. DOI: https://doi.org/10.1002/aoc.1441. (c) Tarassoli A.; Asadi, P.B.; Hitchcock, P.B. *J. Organomet. Chem*. **2006**, *691*, 1631-1636. DOI: https://doi.org/10.1016/j.jorganchem.2005.11.060.
25. Van Der Walt, H.; Muller, A.; van Zyl, W.E. *Acta Crystallogr. Sect. E Struct. Rep. Online*. **2010**, *66*, 2146. DOI: https://doi.org/10.1107/S1600536810029703.
26. Wolf, S.K.; Grimwood, D.J.; McKinnon, J.J.; Turner, M.J., Jayatilaka D., Spackman, M A. Crystal Explorer ver, 3.1, University of Western Australia Perth, **2013**.
27. (a) Gielen, M.; Biesemans, M.; Willem, R. *Appl. Organomet.Chem.* **2005**, *19*, 440–450. DOI: https://doi.org/10.1002/aoc.771. (b) Tiekink, E.R.T. *Appl. Organomet. Chem.* **2008** *22* 533–550. DOI:

ISSN-e 2594-0317

https://doi.org/10.1002/aoc.1441. (c) Pachwania, S.; Devi, J.; Taxak B.; Boora A. *Phosphorus Sulfur Silicon Relat. Elem.* **2022**, *198*, 102-113. DOI: https://doi.org/10.1080/10426507.2022.2116637.

28. (a) Antonenko, T.A.; Gracheva, Y.A.; Shpakovsky, D.B.; Vorobyev, M.A.; Mazur, D.M.; Tafeenko, V.A.; Oprunenko, Y.F.; Shevtsova, E.F.; Shevtsov, P.N.; Nazarov, A.A.; *et al. Int. J. Mol. Sci.* **2023**, *24*, 2024. DOI: https://doi.org/10.3390/ijms24032024. (b) Shiva Prasad, K.: Shiva Kumar, L.; Melvin Prasad; Hosakere D. Revanasiddappa Bioinorg. *Chem. Appl.* **2010**, 854514. DOI: https://doi.org/10.1155/2010/854514.
29. Becker, K.; Heilmann, C.; Peters, G. *Clin. Microbiol. Rev.* **2014** *27*, 870–926. DOI: https://doi.org/10.1128/CMR.00109-13.
30. (a) Ruiz de Gopeguia E. *et. al. Enferm. Infecc. Microbiol. Clin.* **2011**, *29*, 339-344. DOI: https://doi.org/10.1016/j.eimc.2011.02.001. (b) de Almeida L. M. *et al. Antimicrob. Agents Chemother*. **2013**, 4082-4083. https://doi: 10.1128/AAC.00437-1.
31. Carvajal-Román, L. F. *Caracterización estructural de complejos de triorganoestaño (IV) utilizando un ligante ditiofosfonato con una molécula biológicamente activa (colesterol)*; Bachelor's Thesis, Universidad Autónoma del Estado de Morelos. http://riaa.uaem.mx/handle/20.500.12055/4494.